한국해양공학회지 제15권 제2호, pp 22~32, 2001 (ISSN 1225-0767)

Resonance and Response of the Submerged Dual Buoy/Porous-Membrane Breakwaters in Oblique Seas

S. T. KEE
Dept. of Civil Eng., Seoul National University of Technology, Seoul, Korea

KEY WORDS: flexible porous membrane, submerged/floating breakwater, wave-flexible structure interaction, mooring lines, oblique waves, boundary element method

ABSTRACT: *The numerical investigation of obliquely incident wave interactions with fully submerged dual buoy/porous-membrane floating breakwaters placed in parallel with spacing is studied based on linear potential theory and Darcy's law. The numerical solutions are obtained by using a discrete-membrane dynamic model and second-kind modified Bessel function distribution over the entire boundaries of fluid regions. First, numerical solutions for an idealized dual submerged system without buoys are obtained. Second, a more practical dual submerged system with membrane tension provided by buoys at its tops is investigated by the multi-domain boundary element method particularly devised for dual buoy/porous-membrane problems with gaps. The velocity potentials of wave motion are coupled with porous-membrane deformation, and solved simultaneously since the boundary condition on porous-membrane is not known in advance. The effects of varying permeability on membranes and wave characteristics are discussed for the optimum design parameters of systems previously studied. The inclusion of permeability on membrane eliminates the resonances that aggravate the breakwater performance. The system is highly efficient when waves generated by the buoys and membranes were mutually canceled and its energy at resonance frequency dissipates through fine pores on membranes.*

INTRODUCTION

Floating flexible membrane breakwater has the desirable characteristics of being transportable, relatively inexpensive, reusable or sacrificial, and rapidly deployable. Thus it may be an ideal candidate as a portable temporal breakwater for the protection of various coastal/offshore structures and sea operations requiring relatively calm sea states (e.g. Fowler *et al,* 1996).

In this regard, Thompson *et al.,* (1992), Aoki *et al.,* (1994), Kim & Kee (1996), Williams (1996), Kee & Kim (1997), Cho *et al.,* (1997, 1998) investigated the performance of vertical-flexible membrane breakwaters. Kee & Kim (1997) have developed a theory and numerical solution for a surface-piercing or fully submerged and mechanically coupled system. A series of experiments for a surface piercing or a fully submerged system was conducted in a two-dimensional wave tank. The comparison of numerical estimates and experimental result shows the coming wave reflecting performances of those systems were reasonably predicted by the developed theory. Cho *et al.,* (1997, 1998) investigated the performance of a buoy/membrane wave barrier for obliquely incident waves. They expanded the analytical and numerical techniques developed in the previous research to dual systems for surface-piercing or submerged dual membrane idealized wave barriers and more practical dual buoy/membrane wave barriers in the oblique seas. It is found that the efficiency of a dual membrane breakwater can be significantly enhanced compared to the single buoy/membrane system case if it is properly designed. It is also found that the asymmetric system can function better than the symmetric system through desirable tuning.

Chwang (1983) developed a porous wavemaker theory to study the problem of the generation of water waves by the harmonic oscillation of thin permeable plate immersed in water of finite depth, and found that the porous effects reduces not only the wave amplitude but also the hydrodynamic force acting on the wavemaker. Yu and Chawang (1994) investigated numerically the problem of reflection and transmission of water waves by a horizontally submerged plate in water of finite depth, and found that a plate with proper porosity can suppress significantly the wave reflection. Cho and Kim (2000) studied the interaction of monochromatic incident waves with a horizontal porous flexible membrane in the context of two-dimensional linear hydro-elastic theory, and found that the overall performance of the horizontal flexible membrane can be further enhanced by using a proper porous material.

Ideally, the breakwater should have minimum transmission at lee side. It is also often desirable that the reflection should be small. In addition the breakwater has to be submerged in order to reduce the

hydrodynamic pressure on the body of structures, and insure the water circulation to prevent stagnation and pollution in the sheltered region. In this point of view, the performance of the fully submerged floating buoy/porous-membrane breakwaters is investigated for arbitrary incident wave angles and for various permeability on membranes. This breakwater system is able to reduce reflection and transmission simultaneously, and is a very eco-friendly system. The fully submerged system allows gaps to exist over and beneath the structures hinged at some distance over sea bottom, which enables wave transmission through the gaps. The obliquely incident surface waves traveling over long horizontal submerged cylindrical buoy can be trapped inside of the dual system, which act as wave scatterer reducing the wave amplitude, and excites the energy dissipation through fine-pores on membranes.

To assess the efficiency of this dual submerged porous-flexible system, two-dimensional multi-domain hydro-elastic formulation was carried out in the context of linear wave-body interaction theory and Darcy's law. It is also assumed, for simplicity, which the buoy is rigid and the heave motion of the buoy is negligible due to large initial tension. The membrane connecting the buoy and seabed or hinge at some distance above the seabed is assumed to be thin, inextensible, and free to move in the transverse direction while remaining uniform in the longitudinal direction. The coupling of buoy and membrane motions was taken into consideration through an appropriate boundary condition at the joint. The hydrodynamic interaction of oblique incident waves with the combination of the rigid and porous-flexible bodies was solved by the distribution of the simple sources (modified Bessel function of the second kind) that satisfy the Helmholz governing equation. The velocity potentials of wave motion are fully coupled with membrane deformation and porous damping based on Darcy's law.

THEORY AND NUMERICAL METHOD

We consider the interaction of dual floating buoy/porous-membrane wave barrier with obliquely incident waves. An inertial, Cartesian coordinate system (x, y) with its origin located at the still water level is used as reference system. As shown in Fig. 1, the submerged dual system is composed of fully submerged buoy/vertical-flexible-porous-membrane placed in parallel with spacing, and allows flow passing over and beneath structures. The front submerged breakwater is situated at $x=0$, and the second one is situated $x=d_c$, and both breakwaters are assumed to be extendable infinitely in the z-direction. The integration fluid domain is subdivided into three domains. A plane monochromatic incident wave train with small amplitude A and harmonic motion of frequency ω propagates towards the breakwater with an angle θ (wave heading) with respect to x axis in water of constant depth h. For ideal fluids, the wave field may be represented by a velocity potential of an oblique wave $\Phi(x,y,z,t)=Re[\{\phi_o(x,y)+\phi(x,y)e^{ik_z z-i\omega t}]$, where Re denotes the real part of a complex expression, $i=\sqrt{-1}$, t denotes time, and $k_z=k_0\sin\theta$ is the wave number component in the z direction, and k_0 is the wave number of the incident wave, which is the positive real solution of the dispersion equation $\omega^2=k_0 g\tanh k_0 h$ with g being the gravitational coefficient. Then, the velocity potential of small amplitude of wave train height A, wavenumber k_0, and wave heading θ is given by

$$\phi_o=\frac{igA}{\omega}\frac{\cosh k_o(y+h)}{\cosh k_o h}e^{ik_o\cos\theta x} \tag{1}$$

ϕ_0 is the known incident potential and ϕ is the time-independent unknown scattered potential, which includes both diffraction and radiation effects. The complex velocity potentials, ϕ_l in three fluid domains $l=1,2,3$ (see Fig. 1.), satisfy the Helmholtz equation as governing equation and the following linearized free-surface (Γ_F), bottom (Γ_b), and Sommerfeld radiation conditions(Γ_C):

$$\nabla^2\phi_l-k_z^2\phi_l=0 \quad , \quad (l=1,2,3) \tag{2}$$

$$-\omega^2\phi_l+g\frac{\partial\phi_l}{\partial y}=0 \qquad (on\ \ \Gamma_F) \tag{3}$$

$$\frac{\partial\phi_l}{\partial n}=0 \qquad (on\ \ \Gamma_b) \tag{4}$$

$$\lim_{|x|\to\infty}\left(\frac{\partial}{\partial x}\pm ik_x\right)(\phi_l)=0 \quad (on\ \ \Gamma_c\ ,\ l=1,3) \tag{5}$$

where Γ_C is the vertical truncation boundaries at far fields and $n=(n_x,n_y)$ is the unit outward normal vector. Along the vertical fictitious boundaries (matching boundaries) in fluids $x=0$ and $x=d_c$ the pressure and normal velocity are required to be continuous as follows;

$$\phi_l=\phi_{l+1},\quad \frac{\partial\phi_l}{\partial x}=-\frac{\partial\phi_{l+1}}{\partial x} \qquad at\ \Gamma_f \tag{6}$$

Based on Darcy's law the normal velocity inside of membrane with fine pores is linearly proportional to the pressure difference between the two sides of the membrane (Chwang 1983).

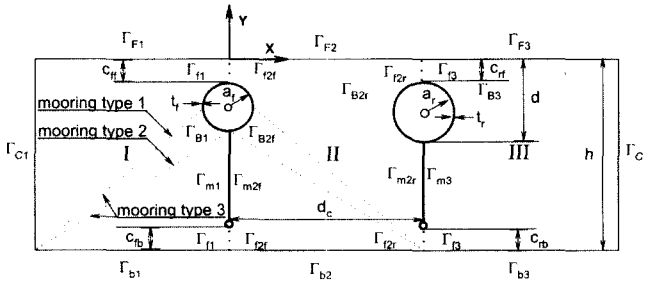

Fig. 1 Coordinate system and integration domains for dual fully submerged buoy/porous membrane breakwater

$$W(y,t)=\frac{B}{\mu}(p_1-p_2)=\frac{B}{\mu}\rho i\omega(\phi_l-\phi_{l+1})e^{-i\omega t}=w(y)e^{-i\omega t}$$
$$at\quad x=0,d_c \tag{7}$$

The scattered potentials must satisfy the following linearized kinematic boundary conditions on the membrane surface:

$$\frac{\partial\phi_l}{\partial x}=-\frac{\partial\phi_{l+1}}{\partial x}=-i\omega\xi+w(y)=-i\omega\xi+\frac{B}{\mu}\rho i\omega(\phi_l-\phi_{l+1}) \tag{8}$$

where μ is constant coefficient of dynamic viscosity, ρ is constant fluid density, and B is a material constant called permeability having the dimension of a length, and the harmonic membrane motions $\Xi(y,t)=Re[\xi(y)e^{ik_z z-i\omega t}]$ in Eqs. (7)~(8). For simplicity, the heave motion of the buoy is assumed to be negligible under large initial tension of membrane. Then the boundary condition on the floating buoy is

$$\frac{\partial\phi_l}{\partial n}+i\omega\{\eta_1 n_x+\eta_3 n_\theta\}+\frac{\partial\phi_o}{\partial n}=0\ ,\quad l=1,2,3\ (on\ \Gamma_B) \tag{9}$$

where $n_\theta=xn_y-yn_x$. To solve the present boundary value problem, a three-domain boundary integral equation method using simple sources along the entire boundary is developed, which can be used for arbitrary bottom topography. Two auxiliary vertical boundaries (Γ_C) are located sufficiently far from the membrane such that the radiation condition (5) is valid.

The fundamental solution (Green function) of the Helmholtz Eq. (2) is $G=-(1/2\pi)K_0(k_z r)$. Here $K_0(k_z r)\approx-\gamma-\ln(k_z r/2)$ is the modified zeroth-order Bessel function of the second kind, and r is the distance from the source point (x',y') to the field point (x,y). As $r\to 0$, one obtains the asymptotic behavior, where $\gamma=0.5772$ is known as Euler's constant. Using recurrence formula $K_0'(u)=-K_{v-1}(u)-(v/u)K_v(u)=(v/u)K_v(u)-K_{v+1}(u)$, the normal derivative of G is given by $\partial G/\partial n=(1/2\pi)k_z K_1(k_z r)\partial r/\partial n$.

Applying Green's second identity in each of the domains to the unknown potentials ϕ_l and imposing the relevant boundary conditions Eqs. (3)~(9), the integral equations in each fluid domain can be written as

$$C\phi_l+\int_{\Gamma_F}[k_z K_1(k_z r)\frac{\partial r}{\partial n}-vK_0(k_z r)]\phi_l d\Gamma$$
$$+\int_{\Gamma_C}[k_z K_1(k_z r)\frac{\partial r}{\partial n}-ik_x K_0(k_z r)]\phi_l d\Gamma$$
$$+\int_{\Gamma_B}[\phi_l k_z K_1(k_z r)\frac{\partial r}{\partial n}+i\omega K_0(k_z r)(\eta_1 n_x+\eta_3 n_\theta)$$
$$+K_0(k_z r)\frac{\partial\phi_0}{\partial n}]d\Gamma$$
$$+\int_{\Gamma_w}[\phi_l\{k_z K_1(k_z r)\frac{\partial r}{\partial n}-s_l\frac{B}{\mu}i\rho\omega K_0(k_z r)\}$$
$$+s_l\frac{B}{\mu}i\rho\omega K_0(k_z r)\phi_{l+1}+s_l(i\omega\xi)K_0(k_z r)]d\Gamma$$
$$+\int_{\Gamma_b}\phi_l k_z K_1(k_z r)\frac{\partial r}{\partial n}d\Gamma=0\qquad(l=1,2,3) \tag{10}$$

where $v=\omega^2/g$ is the infinite-depth wave number, C= solid-angle constant, $s_l=1$, $s_3=-1$, and the integral covers the entire boundary of each fluid region. In Eq. (10), all the boundary conditions of ϕ_l except for the dynamic boundary conditions of buoy and membrane can be straightforwardly implemented. In fluid domain II geometries of half front buoy and half rear buoy exist. In addition backward side of front membrane and forward side of rear membrane is coexist with spacing d_c. In domain II $s_2=-1$, and $s_2=1$ are for backward side of front membrane and forward side of rear membrane respectively.

The integral Eq. (10) should be coupled with the equations of motion of the membranes ξ and buoys η_1, η_3. In addition, the disturbance potentials must satisfy the following linearized dynamic boundary conditions on the membrane surface:

$$\frac{d^2\xi}{dy^2}+\lambda^2\xi=-\frac{\rho i\omega}{T}(\phi_i-\phi_{i+1})\qquad(on\ \Gamma_m) \tag{11}$$

where $\lambda=w\sqrt{m/T}$ with T and m being the membrane tension and mass per unit length respectively. For a numerical approach the discrete form of the equation of membrane motion for $j-th$ element is given by

$$\rho i\omega(\phi_{l(j)}-\phi_{l+1(j)})l_j-T_{(j)}\left(\frac{\partial\xi}{\partial\zeta}\right)_j+T_{(j+1)}\left(\frac{\partial\xi}{\partial\zeta}\right)_{j+1}$$
$$=-ml_j\omega^2\xi_{(j)} \tag{12}$$

where $(\partial\xi/\partial\zeta)_j=(\xi_{f(j)}-\xi_{f(j-1)})/\triangle\zeta_j$, l_j is the length of the $j-th$ segment, and $\triangle\zeta_j=(l_j+l_{j+1})/2$. The geometric boundary conditions at the seabed and the top connection points of membrane $(0,-r_c)$ are $\xi=0$ at $y=-h$, $\xi=\eta_1+R\eta_3$ at $y=-r_c$. R is distance from the connection point $(0,-r_c)$ to rotation center of buoy.

Next, we consider the rigid-body motion of a buoy. As mentioned before, it is assumed that the heave response is negligible due to large initial tension. The coupled equations of motion for sway and roll are given by

$$M(-\omega^2)X=F_p-(K_{HS}+K_m)X-F_T+F_D \tag{13}$$

where X is displacement of sway and roll, M is a mass matrix of buoy, F_p is hydrodynamic forces and moments on buoy, K_{HS} is the restoring forces and moments due to the hydrostatic pressure,

K_m is sway and roll mooring stiffness coefficients including the effects of pretension, F_D is the nonlinear viscous drag force, and these are detailed in Kee & Kim (1997). The symbol F_T is forces and moments on the buoys caused by the initial tension of membrane at the connection points between membranes and buoys.

$$F_T = T_{(N_m+1)} \begin{Bmatrix} -\sin\alpha \\ R\sin\eta_3\cos\alpha - R\cos\eta_3\sin\alpha \end{Bmatrix} \tag{14}$$

where α is the angle of membrane at the connections with respect to the y axis and the symbol R is the radial distances from the center of rotation of buoy to the connection point on buoy. Assuming the angle α is small, then $\cos\alpha \cong 1$, $\sin\alpha \cong -(\partial\xi/\nabla\zeta)_{N_m+1}$, and Eq. (14) can be rewritten as

$$F_T = T_{(N_m+1)} \begin{bmatrix} \frac{2}{l_{N_m}} & \frac{2R}{l_{N_m}} \\ \frac{2R}{l_{N_m}} & R+\frac{2R^2}{l_{N_m}} \end{bmatrix} \begin{Bmatrix} \eta_1 \\ \eta_3 \end{Bmatrix} - T_{(N_m+1)} \begin{bmatrix} \frac{2}{l_{N_m}} \\ \frac{2R}{l_{N_m}} \end{bmatrix} \xi_{N_m} \tag{15}$$

This equation is composed of two terms: the first term is positive restoring forces and moments to the each buoy, and the second term is excitation force proportional to the motion amplitude of the neighboring membrane element. Therefore, the membrane tensions can be either restoring forces or excitations.

So far, we have obtained integral Eq. (10) for ϕ_l, $l=1,2,3$, and equation of membrane motion (12) and equations of buoy motions (13). They are mutually coupled, so they need to be solved simultaneously. If we discretize fluid domain 1 and 3 by $NE_{1,3}$ segments, and discretize middle domain 2 by NE_2, we have $2NE_{1,3}+NE_2$ unknowns for ϕ_1, ϕ_2, and ϕ_3, $N_{mf}+N_{mr}$ unknowns for ξ_f and ξ_r, and four more unknowns η_{f1}, η_{f3} and η_{r1}, η_{r3}, where the sub notations f, r mean front and rear respectively. Therefore, we have to solve NT number of linear simultaneous equations. Here the numbers of $NE_{1,3}$, NE_2, NT is given by

$$NE_{1,3} = N_F + N_C + N_b + N_{mf} + N_{mr} + N_{Bf} + N_{Br}$$
$$NE_2 = N_F + N_b + N_{mf} + N_{mr} + N_{Bf} + N_{Br}$$
$$NT = 2NE_{1,3} + NE_2 + N_{mf} + N_{mr} + 4$$

NUMERICAL RESULTS AND DISCUSSIONS

The three-domain boundary element program has been developed based on linear potential theory and Darcy's law as described in the preceding section, and was used to demonstrate the performance of fully submerged dual buoy/porous-membrane floating breakwaters in oblique seas. The membrane is assumed to be thin and inextensible. It is also assumed that the initial membrane tension is large such that heave motions are small compared to other responses and dynamic tension is much smaller than the static tension. The computational domain is defined as in Fig. 1. The two submerged system is situated in parallel with spacing d_c. The submerged buoy/porous-membrane system allows gap c_{ff}, c_{fb}, c_{rf}, c_{rb}, which present front free surface gap, front bottom gap, and rear free surface gap, rear bottom gap respectively. The truncation boundary is located 3-4 water depth away from the membrane to ensure that local wave effect is negligible.

When the buoy is absent or negligibly small, the convergence of the results with increasing the number of segments is also shown in Figs. 3a~3b. for porous membrane system with permeability B=5E-08. It is seen that the errors uniformly converges as the number of segments is increased. The error (%) was calculated from the energy conservation relation $R_f^2 + T_r^2 = 1$. For a non-porous system the energy relation has to be satisfied to be near zero error, but for a porous system it cannot be satisfied due to energy dissipation. From this test, the number of total elements in the half fluid domain $N=250$ gave sufficient accuracy and thus was used for the ensuing computation. For the present numerical results, viscous drag forces F_D are not included unless mentioned otherwise.

As coordinate system and computational domain are defined in Fig. 2, the two submerged membrane system in parallel with spacing and gaps. The convergence test of the developed BEM program has been done for the system design parameter $\bar{T}=0.255$, $c_{ik}/h=0.125$, $d_c/h=1$ Figs. 3c~3f. shows the results with increasing the permeability coefficient B=0, 1E-09, 5E-09, 1E-08, 5E-08, 1E-07, 5E-07, 1E-06. $\bar{T}$ is non-dimensional tension of membrane by $(T/\rho gh^2)$. Figs. 3c~3d. shows transmission coefficient T_r as function of kh. The transmitted

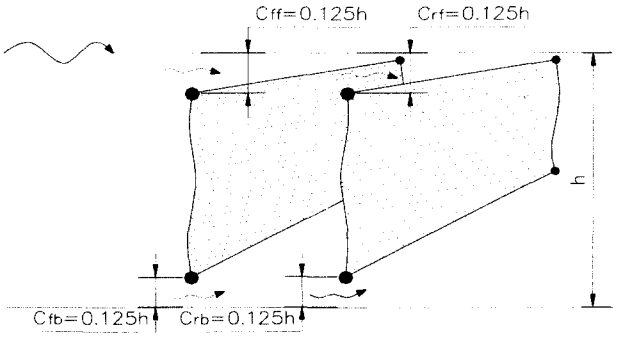

Fig. 2 Definite sketch of dual submerged permeable membrane breakwater

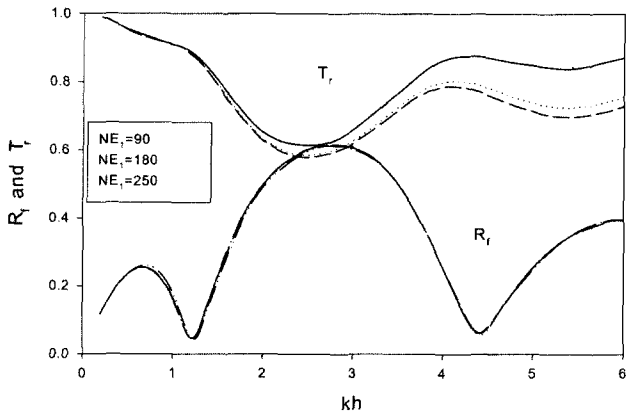

Fig. 3a Reflection and transmission coefficients for $c_{ik}/h=0.125$, $\bar{T}=0.255$ as function of kh with varying $NE_1=90,180,250$

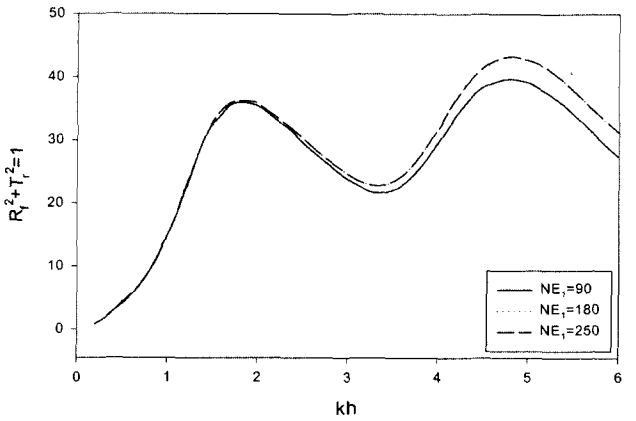

Fig. 3b Energy relation error for the convergence test of BEM for $c_{ik}/h=0.125$, $\bar{T}=0.255$ as function of kh with varying $NE_1=90,180,250$

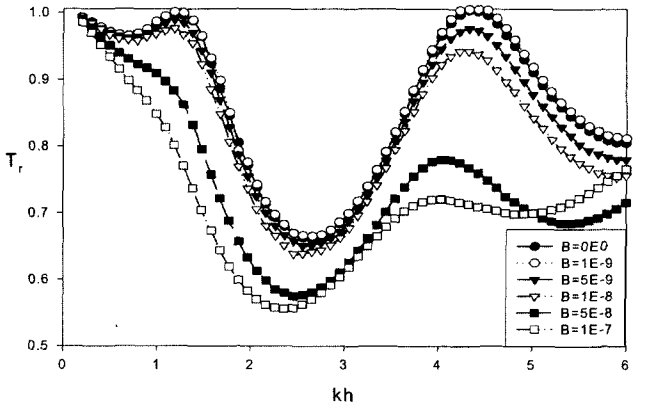

Fig. 3c Convergence test; Transmission coefficients of varying permeability of membrane for $c_{ik}/h=0.125$, $d_c/h=1$, $\bar{T}=0.255$, $B=0E-0\sim1E-7$

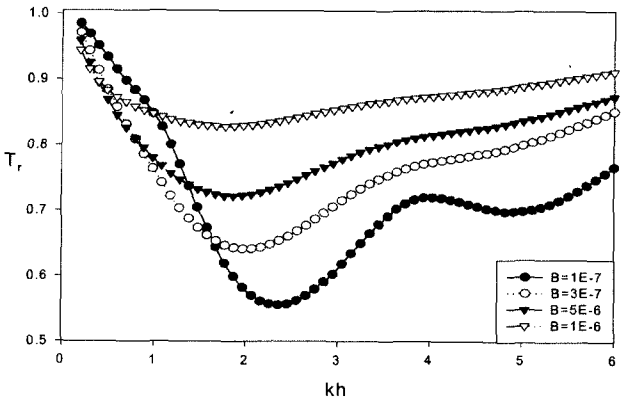

Fig. 3d Convergence test; Transmission coefficients of varying permeability of membrane for $c_{ik}/h=0.125$, $d_c/h=1$, $\bar{T}=0.255$, $B=1E-7\sim1E-6$

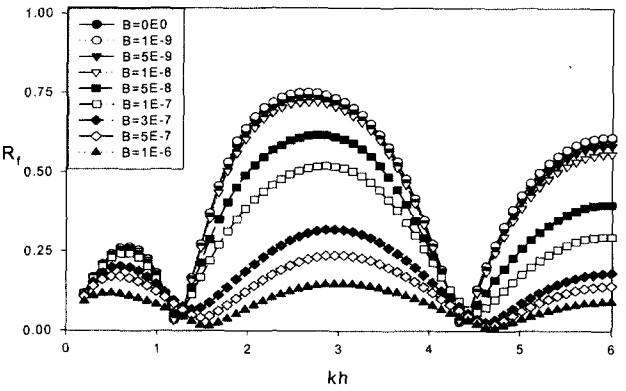

Fig. 3e Convergence test; Reflection coefficients of varying permeability of membrane for $c_{ik}/h=0.125$, $d_c/h=1$, $\bar{T}=0.255$

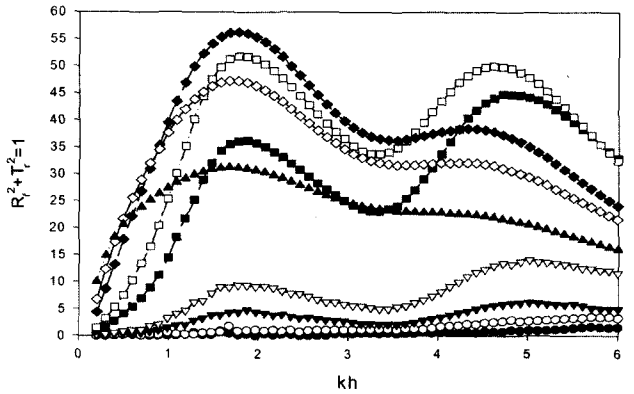

Fig. 3f Convergence test; Energy relation coefficients of varying permeability of membrane for $c_{ik}/h=0.125$, $d_c/h=1$, $\bar{T}=0.255$
; the plotted line and symbols is equivalent to those of Fig. 3e

wave is gradually reduced as B increases in Fig. 3a. When B increase further over 1E-07, transmitted wave is increased. The turning frequency from decreased transmission to increased transmission migrates toward high frequency from $kh=1.6$ up to $kh=0.2$ as B increased further. Fig. 3e. shows wave reflection coefficients converged continuously according to the various B values. Fig. 3f. shows the energy relation error (%) with respect to varying B values. It is interesting that the limit value of B for maximum energy dissipation exist over all frequencies $kh=0.2\sim6$ for beam seas. When B is greater than 1E-07, the energy dissipation effects starts to be diminished at $kh=4.2$, and gradually reduced over all frequency band as B further increased.

The comparison of performances for an ideal dual submerged membranes wave barrier of $\bar{T}=0.225$, $c_{ik}=0.125$, $d_c/h=1$ with and without permeability is presented in Figs. 4a~4b. as function of kh and θ. In the oblique seas, the effective wavelength in the x-direction becomes shorter and submerged systems with or without permeability (B=1E-07) turns out to be little effective. When narrow gaps are allowed over and beneath membrane, rapid variations of the potential flow near the gaps are expected. In addition the front membrane motion in vertical sinusoidal manner generates local standing waves, which is exponentially decaying in the x-direction in the lee side. When the initial tension is relatively large, gap is not small compared to wave length, the positive effects of membrane hydrodynamics is diminished for the shorter wavelength in oblique sea.

In reality, the buoyancy force of buoys can easily provide the external tensions in membrane. However, the presence of large buoys can significantly change the scattered wave field. In addition the permeability on membrane dissipates the fluctuations by re-reflected and radiated waves between two submerged vertical systems, and behaves as dampers with relevant to its velocity. Therefore physical phenomena of oblique wave interaction with submerged buoy/porous-membrane dual systems are quite complicated.

The convergence test for the submerged dual buoy/porous-membrane BEM code shows, in Figs. 5a~5b, that permeability of membrane can enhance the efficiency only at the limited range of frequencies. As B increased, the transmitted wave is decreased at some region of frequencies $kh=0.2\sim1.5$ and $kh=5.\sim6.$, and the transmitted wave is increased at $kh=3.5\sim5.0$ as shown in Fig. 5a. As B increase, the reflection coefficient is gradually reduced up to B=1E-08, and starts to increase in Fig. 5b. It means that the hydrodynamic effects by membrane motions in vertical sinusoidal manner are less than that of buoys for dual system with highly permeable membranes.

The performance of dual submerged buoy/solid-membrane floating wave barriers for $T_i/K_{i1}=0$, $T_i/K_{i2}=0.1$, $t_i/a_i=0.02$, $a_i/h=0.2$, $c_{ik}/h=0.05$, $d_c/h=1$ is shown in Figs. 6a~6b. These two systems have same design parameters, and allow semi-pivotal motions of buoys with only joint moorings. Thus we can observer several resonance in the performances, in which will be subsequent to system failure or give severe damages on the integrity of structures. After putting a permeability B=3E-08 on the membranes, the resonance is quite diminished in transmission and reflection as shown in Figs. 7a~7b. The amplitudes of buoy/porous-membrane motion or forces on membranes are also of practical interest and shown in Figs. 8~15. for the given system. Figs. 8a~8b. show the profiles of the non-dimensional membrane response amplitudes (per unit incident wave amplitude as function of kh and vertical position y/h for beam seas. As expected, the response amplitude sharply increased at resonance frequencies, which generate large propagating waves in lee side. It is interesting that motion amplitude of rear membrane for $\theta=0^\circ$ is quite small compare to that of front one, just except the frequencies near resonance and low and high frequencies. The motion amplitudes of front and rear membrane at these resonance frequencies is similar to each other in their magnitudes. It is also interesting that response of rear membrane for $\theta=45^\circ$ is a plane flat, so that it shows a good performance for wide range of kh except two resonances in Fig. 9. The local force distribution for rear membrane is shown in Fig. 10, and we can see that the force is greatly increased near resonance to cause large membrane responses. We also can observe zero force region and quite asymmetric hydrodynamic pressure distribution in the vicinity of $kh=4.5$. The motion amplitudes of front and rear buoys are shown in Figs. 11~12b, and sway motion amplitude of rear buoy for $\theta=0^\circ$ is small enough for us to see near zero motion at $kh=1.5$. The motion amplitudes of front (Fig. 11.) and rear (Fig. 12a.) buoys at resonance frequencies are similar to each other in their magnitudes. Fig. 12b shows the motion amplitude at joint between buoy and membrane, the amplitudes for $\theta=0^\circ$ can be matched to the amplitudes of rear membrane at highest vertical position y/h in Fig. 8b.

In practice, the amplitudes of buoy/porous-membrane motion are of practical interest and shown in Figs. 13a~13b. and Figs. 15a~15c. And the corresponding T_r, R_f are shown in Fig. 7a~7b. for the given system with permeability B=3E-08 on the membranes. The sharp spikes in motion amplitudes of buoy/membrane are completed eliminated after applying permeability on membranes. The comparison of rear motions for B=0 (Fig. 8b.) and for B=3E-8 (Fig. 13a.) shows that amplitudes at low frequencies is significantly reduced. However, the two peak-motion amplitudes of rear membranes for B=3E-8 (Fig. 13b.) is slightly reduced compared to those for B=0 (Fig. 9.) at the incident wave angle $\theta=45^\circ$. Similar phenomena occur in the comparison of force on membrane and motions at joint.

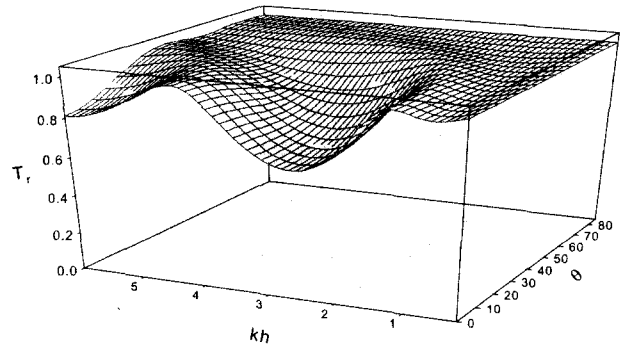

Fig. 4a The transmission coefficients as function of kh and θ for $c_{ik}/h=0.125$, without buoy, $d_c/h=1$, $\bar{T}=0.255$, $B=0E0$

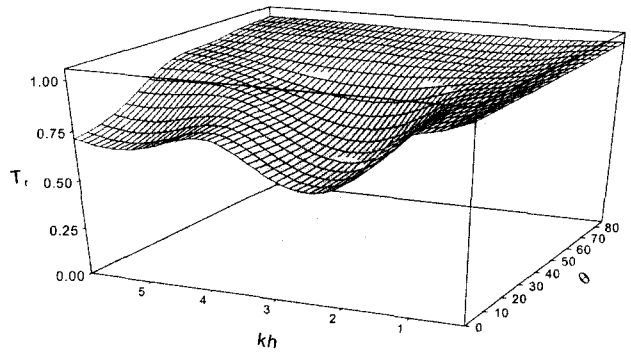

Fig. 4b The transmission coefficients as function of kh and θ for $c_{ik}/h=0.125$, without buoy, $d_c/h=1$, $\bar{T}=0.255$, $B=1E-8$

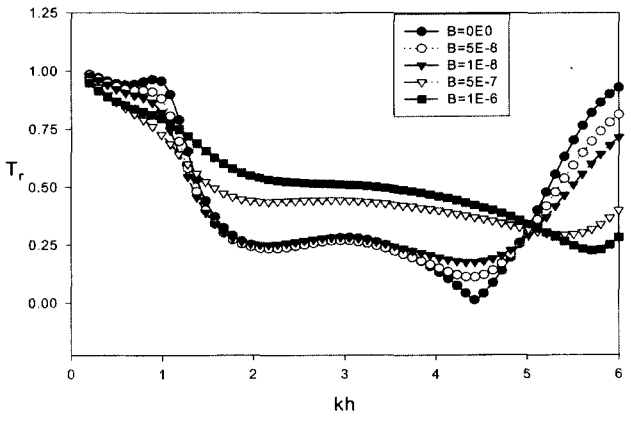

Fig. 5a The transmission coefficients with varying permeability of membrane for $\theta=0°$, $T_f/K_{fj}=0.1$, $T_r/K_{r1}=0$, $T_r/K_{r2}=0.1$, $t_i/a_i=0.02$, $a_i/h=0.2$, $c_{ik}/h=0.125$, $d_c/h=1$

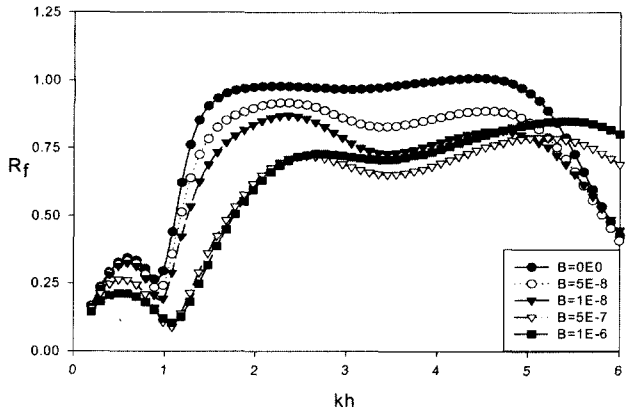

Fig. 5b The reflection coefficients with varying permeability of membrane for $\theta=0°$, $T_f/K_{fj}=0.1$, $T_r/K_{r1}=0$, $T_r/K_{r2}=0.1$, $t_i/a_i=0.02$, $a_i/h=0.2$, $c_{ik}/h=0.125$, $d_c/h=1$

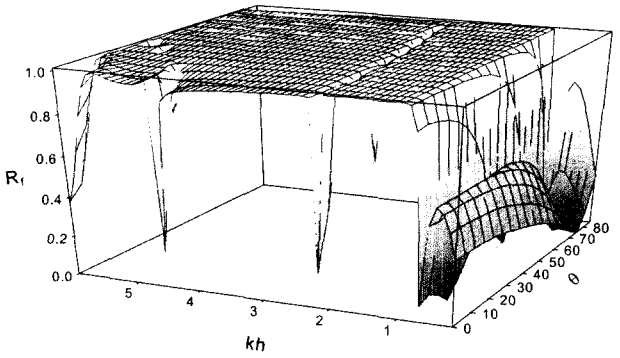

Fig. 6a The reflection coefficients as function kh and θ for $T_i/K_{i1}=0$, $T_i/K_{i2}=0.1$, $t_i/a_i=0.02$, $a_i/h=0.2$, $c_{ik}/h=0.05$, $d_c/h=1$, $E=0E0$

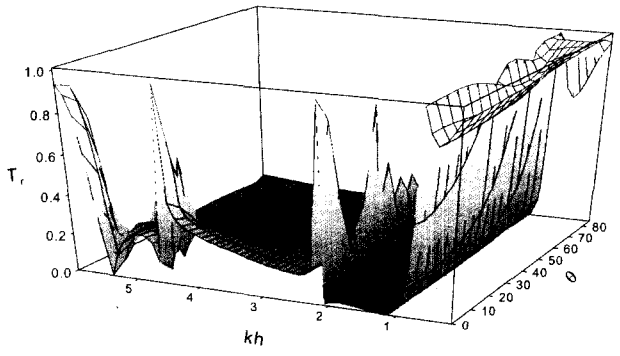

Fig. 6b The transmission coefficients as function kh and θ for $T_i/K_{i1}=0$, $T_i/K_{i2}=0.1$, $t_i/a_i=0.02$, $a_i/h=0.2$, $c_{ik}/h=0.05$, $d_c/h=1$, $E=0E0$

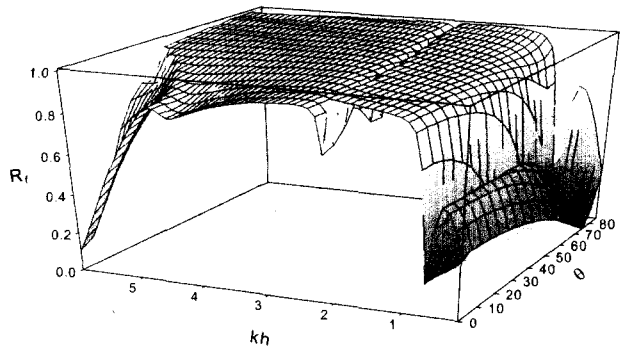

Fig. 7a The reflection coefficients as function kh and θ for $T_{i}/K_{i1}=0$, $T_{i}/K_{i2}=0.1$, $t_{i}/a_{i}=0.02$, $a_{i}/h=0.2$, $c_{ik}/h=0.05$, $d_{c}/h=1$, $E=3E-8$

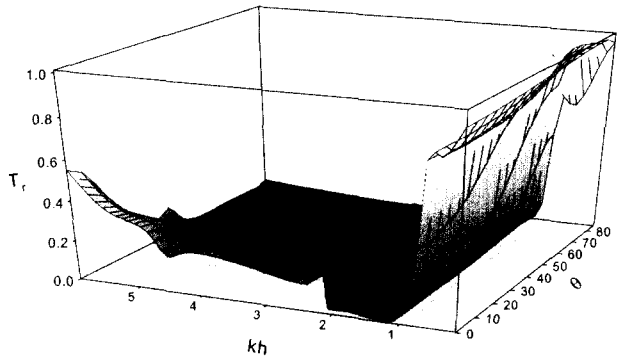

Fig. 7b The transmission coefficients as function kh and θ for $T_{i}/K_{i1}=0$, $T_{i}/K_{i2}=0.1$, $t_{i}/a_{i}=0.02$, $a_{i}/h=0.2$, $c_{ik}/h=0.05$, $d_{c}/h=1$, $E=3E-8$

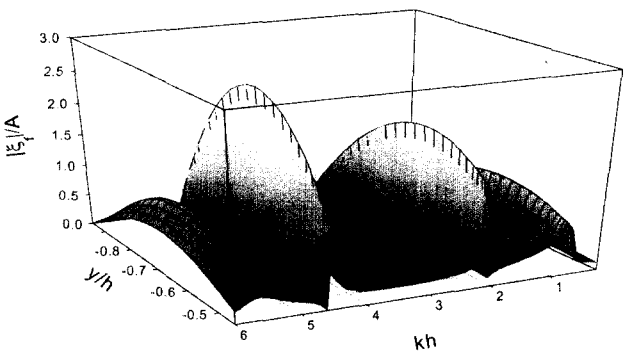

Fig. 8a Response of a front membrane as function of kh and y/h for $\theta=0^{\circ}$, $T_{i}/K_{i1}=0$, $T_{i}/K_{i2}=0.1$, $t_{i}/a_{i}=0.02$, $a_{i}/h=0.2$, $c_{ik}/h=0.05$, $d_{c}/h=1$, $E=0E0$

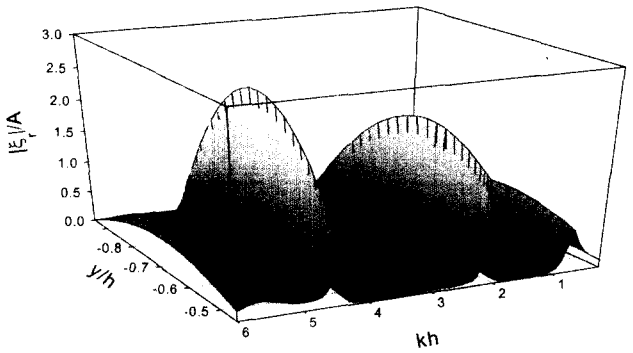

Fig. 8b Response of a rear membrane as function of kh and y/h for $\theta=0^{\circ}$, $T_{i}/K_{i1}=0$, $T_{i}/K_{i2}=0.1$, $t_{i}/a_{i}=0.02$, $a_{i}/h=0.2$, $c_{ik}/h=0.05$, $d_{c}/h=1$, $E=0E0$

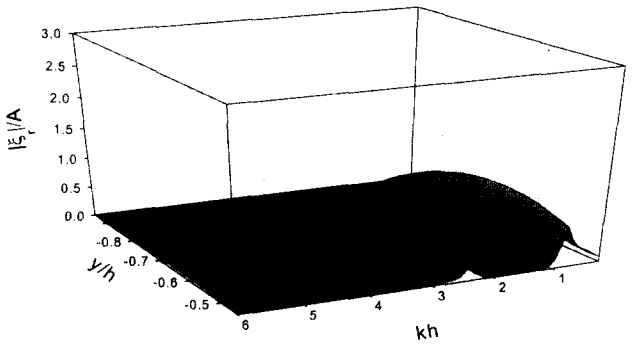

Fig. 9 Response of a rear membrane as function of kh and y/h for $\theta=45^{\circ}$, $T_{i}/K_{i1}=0$, $T_{i}/K_{i2}=0.1$, $t_{i}/a_{i}=0.02$, $a_{i}/h=0.2$, $c_{ik}/h=0.05$, $d_{c}/h=1$, $E=0E0$

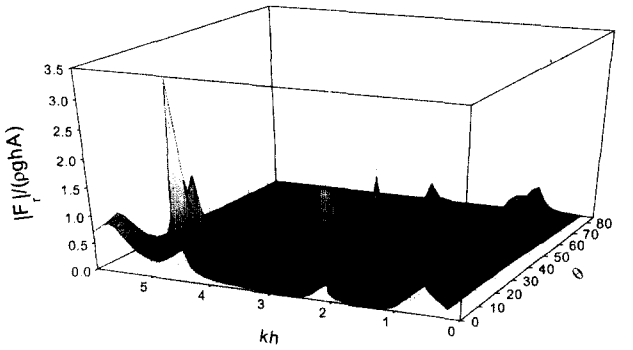

Fig. 10 Force distribution on a rear membrane as function of kh and θ for $T_{i}/K_{i1}=0$, $T_{i}/K_{i2}=0.1$, $t_{i}/a_{i}=0.02$, $a_{i}/h=0.2$, $c_{ik}/h=0.05$, $d_{c}/h=1$, $E=0E0$

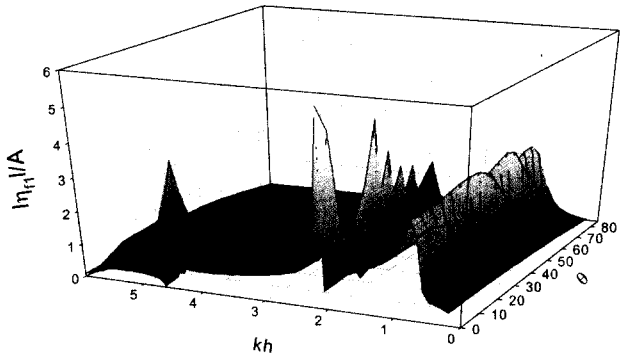

Fig. 11 Sway motion of front cylinder as function kh and θ for $T_i/K_{i1}=0$, $T_i/K_{i2}=0.1$, $t_i/a_i=0.02$, $a_i/h=0.2$, $c_{ik}/h=0.05$, $d_c/h=1$, $E=0E0$

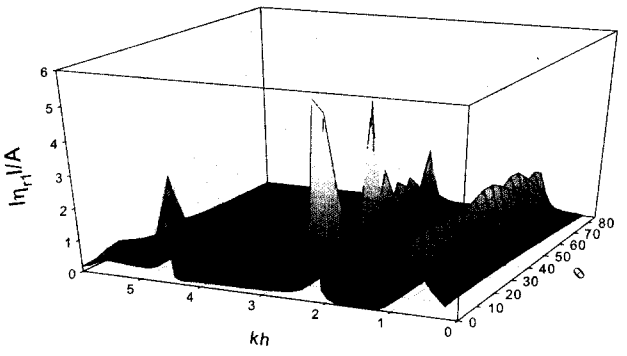

Fig. 12a Sway motion of rear cylinder as function kh and θ for $T_i/K_{i1}=0$, $T_i/K_{i2}=0.1$, $t_i/a_i=0.02$, $a_i/h=0.2$, $c_{ik}/h=0.05$, $d_c/h=1$, $E=0E0$

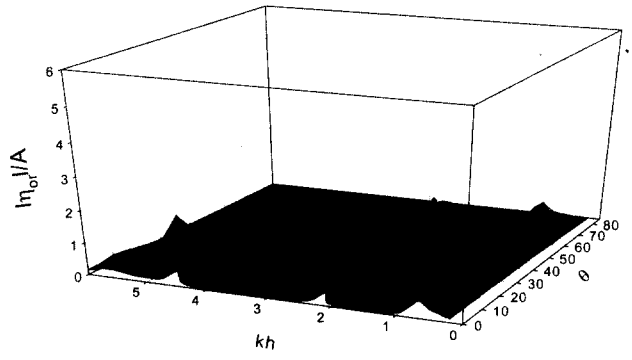

Fig. 12b Joint motion of rear cylinder as function kh and θ for $T_i/K_{i1}=0$, $T_i/K_{i2}=0.1$, $t_i/a_i=0.02$, $a_i/h=0.2$, $c_{ik}/h=0.05$, $d_c/h=1$, $E=0E0$

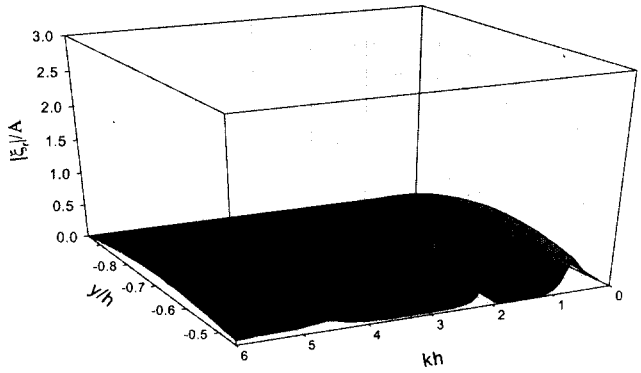

Fig. 13a Responses of a rear membrane as function kh and y/h for $\theta=0°$ $T_i/K_{i1}=0$, $T_i/K_{i2}=0.1$, $t_i/a_i=0.02$, $a_i/h=0.2$, $c_{ik}/h=0.05$, $d_c/h=1$, $E=3E-8$

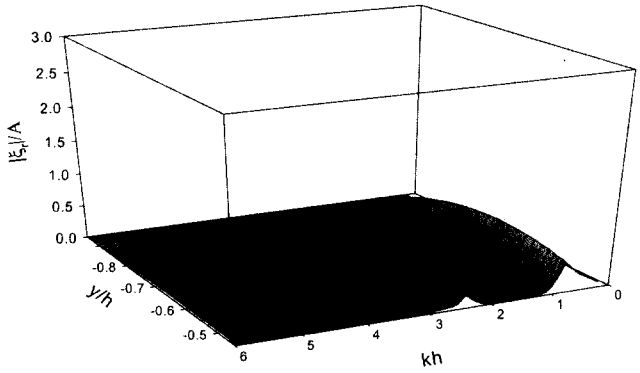

Fig. 13b Responses of a rear membrane as function kh and y/h for $\theta=45°$ $T_i/K_{i1}=0$, $T_i/K_{i2}=0.1$, $t_i/a_i=0.02$, $a_i/h=0.2$, $c_{ik}/h=0.05$, $d_c/h=1$, $E=3E-8$

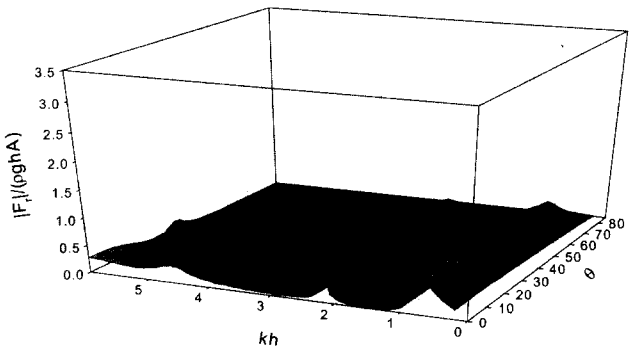

Fig. 14 Force distribution on a rear membrane as function of kh and θ for $T_i/K_{i1}=0$, $T_i/K_{i2}=0.1$, $t_i/a_i=0.02$, $a_i/h=0.2$, $c_{ik}/h=0.05$, $d_c/h=1$, $E=3E-8$

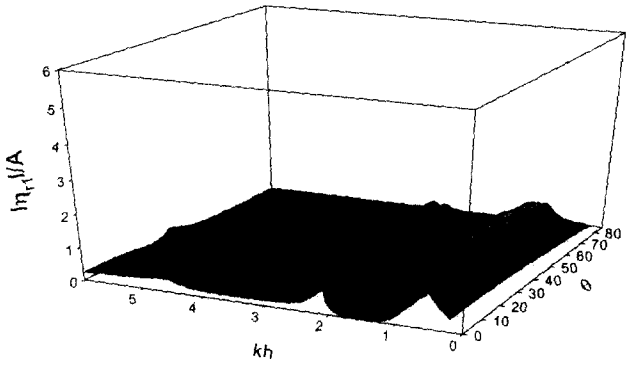

Fig. 15a Sway motion of rear cylinder as function kh and θ for $T_f/K_{f1}=0$, $T_f/K_{f2}=0.1$, $t_f/a_f=0.02$, $a_f/h=0.2$, $c_{fk}/h=0.05$, $d_c/h=1$, $E=3E-8$

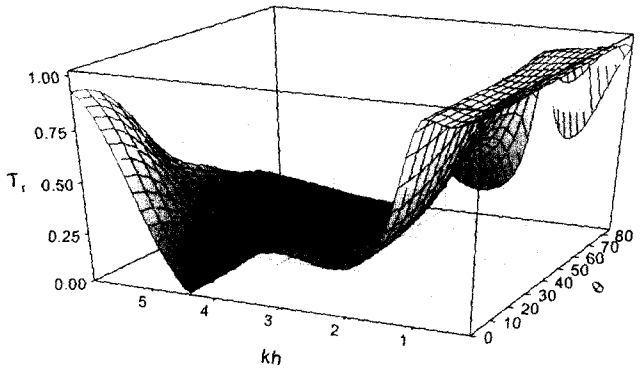

Fig. 16a The transmission coefficients of varying permeability of membrane as function kh and θ for $T_f/K_{f1}=0.1$, $T_r/K_{r1}=0$, $T_r/K_{r2}=0.1$, $t_f/a_f=0.02$, $a_f/h=0.2$, $c_{fk}/h=0.125$, $d_c/h=1$, $E=0E0$

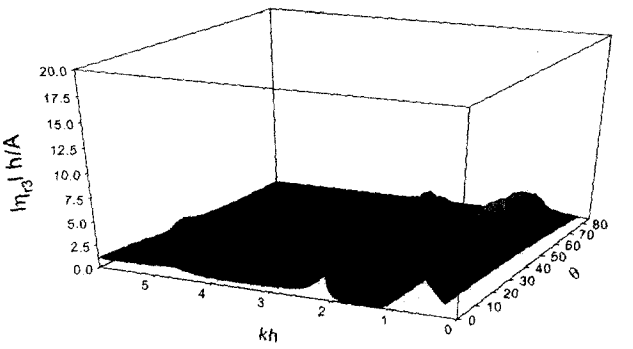

Fig. 15b Roll motion of rear cylinder as function kh and θ for $T_f/K_{f1}=0$, $T_f/K_{f2}=0.1$, $t_f/a_f=0.02$, $a_f/h=0.2$, $c_{fk}/h=0.05$, $d_c/h=1$, $E=3E-8$

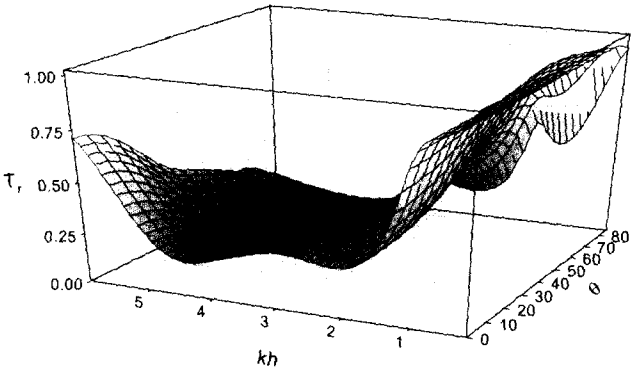

Fig. 16b The transmission coefficients of varying permeability of membrane as function kh and θ for $T_f/K_{f1}=0$, $T_r/K_{r1}=0$, $T_r/K_{r2}=0.1$, $t_f/a_f=0.02$, $a_f/h=0.2$, $c_{fk}/h=0.125$, $d_c/h=1$, $E=1E-7$

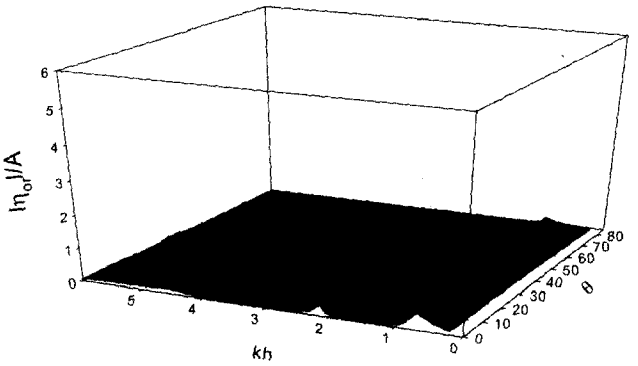

Fig. 15c Joint motion of rear cylinder as function kh and θ for $T_f/K_{f1}=0$, $T_f/K_{f2}=0.1$, $t_f/a_f=0.02$, $a_f/h=0.2$, $c_{fk}/h=0.05$, $d_c/h=1$, $E=3E-8$

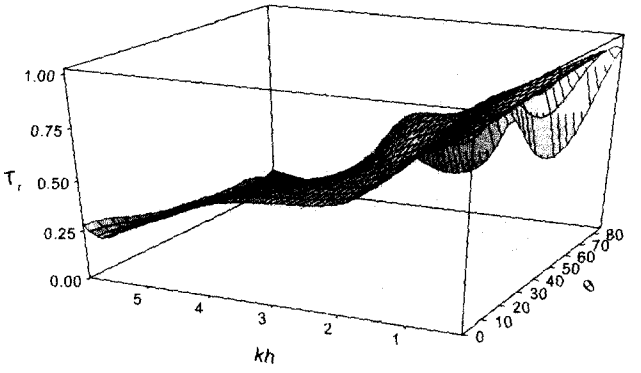

Fig. 16c The transmission coefficients of varying permeability of membrane as function kh and θ for $T_f/K_{f1}=0.1$, $T_r/K_{r1}=0$, $T_r/K_{r2}=0.1$, $t_f/a_f=0.02$, $a_f/h=0.2$, $c_{fk}/h=0.125$, $d_c/h=1$, $E=1E-6$

Finally, Figs. 16a~16c. shows the transmission coefficient as function of non-dimensional frequencies and various wave headings for the various permeability B=0, 1E-07, 1E-06, and for $T_f/K_{f1}=0.1$, $T_r/K_{r1}=0$, $T_r/K_{r2}=0.1$, $t_i/a_i=0.02$, $a_i/h=0.2$, $c_{ik}/h=0.125$, $d_c/h=1$. When the system adopt the permeability coefficient B=1E-07, transmitted waves is decreased for wide range of kh, however, it is increased in the vicinity of $kh=4.5$. For the large permeability coefficient B=1E-06, the transmission still is decreased at the high and low frequency band. However, it is increased at the frequency range of $kh=1.2\sim5$. The performance of this is generally poor for the mid-frequency range and over wide wave headings. Therefore permeability coefficient B=1E-07 seems to be proper to maximize the energy dissipation within dual buoy/porous-membrane systems.

SUMMARY AND CONCLUSIONS

The interaction of oblique incident waves with submerged dual buoy/porous-membrane was solved in the context of two-dimensional linear hydro-elastic interaction theory and Darcy's law. Both the ideal system composed of only submerged dual porous-membrane with spacing and more practical dual submerged buoy/porous-membrane systems were considered. An adjusted three-domain BEM was employed since the membrane is infinitely thin and porous. The solutions of each domain were matched at the respective membrane surfaces. Membrane motions and velocity potentials were solved simultaneously because the body-boundary condition on the porous-membrane is not known in advance, as other hydro elastic problems.

Using the developed program code, the performance of fully submerged dual systems in oblique waves was tested with various breakwater design parameters, wave conditions, and permeability on membranes. From these examples, it is shown that the use of the submerged dual buoy/flexible porous-membranes can significantly increase the overall wave blocking efficiency in normal and oblique incident waves except long wave frequencies. Allowing motion of buoys and membranes, the mutual cancellation effect of incident waves and scattered waves significantly enhance the performance as breakwaters. Applying proper permeability on membrane eliminates resonance of system to secure the safety of structural dynamics, and reduces transmission and reflection. In addition it insure economical manufactures, operation, andmaintains. Using a properly devised asymmetric system, which can complement each other, we can further enhance the efficiency. In most cases, mooring type, gaps, proper permeability, and size of buoy for sufficiently large membrane tension needs to be provided to guarantee high performance over a wide range of wave frequencies.

Using the developed computer program, an optimum design for a given sea condition can be determined through a comprehensive parametric study including various buoy shapes. To see the effects of large motions and high waves, a nonlinear time-domain program needs to be developed.

ACKNOWLEDGMENT

This research was sponsored by the Korea Institute of Construction Technology (KICT) Research Center Program, Grant Number R&F/00-24-01.

REFERENCES

Aoki, S., Liu, H., & Sawaragi, T. (1994). "Wave transformation and wave forces on submerged vertical membrane", Proc. Intl. Symp. Waves - Physical and Numerical Modeling, Vancouver, pp 1287~1296.

Cho, I.H. & Kim, M.H. (2000). "Interactions of Horizontal Porous Flexible Membrane with Waves", ASCE J. of Waterway, Port, Coastal & Ocean Engineering, Vol. 126, No. 5, pp 245~253.

Cho, I.H. & Kee, S.T & Kim, M.H. (1998). "The Performance of Dual Flexible Membrane Wave Barrier in Oblique Sea", ASCE J. of Waterway, Port, Coastal & Ocean Engineering, Jan./Feb. 1998 Vol. 124, No. 1, pp 21~30.

Cho, I.H. & Kee, S.T. & Kim, M.H. (1997). "The Performance of Dual Flexible Membrane Wave Barrier in Oblique Incident Waves", J. of Applied Ocean Research, Jun./Aug. 1997. Vol. 19, No. 3-4, pp 171~182.

Chwang, A. T. (1983). "A porous wavemaker theory", J. Fluid Mech., Cambridge, U.K.,Vol. 132, pp 395~406.

Fowler, J., Resio, D., Briggs, M., Pollock, C. (1996). "Potential uses for rapidly installed breakwater systems", Proc. 12th ICCE Conf., Orlando

Kee, S.T. & Kim, M.H. (1997). "Flexible membrane wave barrier. Part 2. Floating/submerged buoy-membrane system", ASCE J. of Waterway, Port, Coastal & Ocean Engineering, Vol. 123, No. 2, pp 82~90.

Kim, M.H. & Kee, S.T. (1996). "Flexible membrane wave barrier. Part 1. Analytic and numerical solutions", ASCE J. of Waterway, Port, Coastal & Ocean Engineering, Vol. 122, No. 1, pp 46~53.

Thompson, G.O., Sollitt, C.K., McDougal, W.G. & Bender W.R. (1992). "Flexible membrane wave barrier", ASCE Conf. Ocean V, College Station, pp 129~148.

Williams, A.N. (1996). "Floating membrane breakwater", J. of Offshore Mechanics & Arctic Engr., Vol. 118, pp 46~51.

Yu, X., and Chwang, A. T. (1994). "Wave motion through porous structures", J. Engrg. Mech., ASCE, Vol. 120, No. 5, pp 989~1008.

2001년 1월 18일 원고 접수
2001년 3월 25일 수정본 채택